Talanta 219 (2020) 121242

Contents lists available at ScienceDirect

Talanta

journal homepage: www.elsevier.com/locate/talanta

Enzyme-free electrochemical biosensor based on double signal amplification strategy for the ultra-sensitive detection of exosomal microRNAs in biological samples

Wenting Cheng[a,1], Jiehua Ma[b,1], Pu Cao[c], Yongchen Zhang[c], Chuanjun Xu[c], Yongxiang Yi[c,*], Jinlong Li[c,**]

[a] Department of Clinical Laboratory, Nanjing Gaochun People's Hospital, Nanjing, 211300, PR China
[b] Women's Hospital of Nanjing Medical University, Nanjing Maternity and Child Health Care Hospital, Nanjing, 210004, PR China
[c] The Second Hospital of Nanjing, Nanjing University of Chinese Medicine, Nanjing, 210003, PR China

ARTICLE INFO

Keywords:
miRNA
Exosomes
Double signal amplification
Silver nanoparticles

ABSTRACT

Growing evidence suggests that exosomes-encapsulated miRNAs detection is of paramount significance in early diagnostics of cancer due to protection from degradation by ribonuclease. However, exosomal microRNAs with low abundance and subtle variation have restricted their clinical application. Herein, an electrochemical biosensor for highly sensitive detection of exosomal microRNAs has been fabricated based on the double signal amplification strategy. Our proposed amplifier consists of two steps: target miRNA cyclic signal amplification induced by strand displacement reaction (SDR) and subsequent deposition of silver nanoparticles induced by streptavidin-biotin interaction. Consequently, this method shows ultrahigh sensitivity to detect miRNA. Taking miRNA-21 in exosomes as a model analyte, a detection limit of 0.4 fM (S/N = 3) can be obtained. Meanwhile, the method is relatively simple and low-cost without the requirement of enzyme, which has been applied in biological samples successfully. Therefore, our miRNA assay method has shown great promise as molecular tool in the detection of exosomal miRNA and could be widely used in clinic in the future.

1. Introduction

Exosomes are membranous vesicles ranging in size from 30 to 100 nm secreted by almost all types of cells and play key roles as messengers that function in intercellular communication by delivering the information that they carry to the target cells [1,2]. Now exosomes have attracted increasing attention due to their ability to carry a variety of cargoes, including proteins, microRNAs, mRNAs and even DNAs from parental cells, which enables them to maintain physiological functions and involve in the pathogenesis of multiple diseases [3–6]. MicroRNAs (miRNAs) in exosomes play important functions in developmental regulation, proliferation, differentiation, cardiogenesis, epigenetic inheritance and so forth [7,8]. Additionally, there are elevated evidences demonstrating that the aberrant expression of miRNAs has been correlative to various diseases, including a broad range of cancers, heart disease and neurological diseases [9–12]. Due to the outer lipid membrane of exosome, exosomal miRNA are generally protected from degradation by ribonuclease, thereby offering a stable source of miRNA in the peripheral blood. So, assay of exosomal miRNA will provide more useful details of disease diagnosis.

MiRNAs have been regarded as a new branch of diagnostic and prognostic biomarkers for clinical management, and a diversity of techniques are developed for miRNA detection [13–16]. Among them, northern blotting [17,18], real-time PCR [19,20] and microarrays [21,22] are the commonly used strategies. Nevertheless, these methods require tedious sample preparation process and/or a thermal cycler. There are still many other miRNA sensing platforms detecting different kinds of signals, such as surface enhanced raman scattering (SERS) [23,24], electrochemical [25–27], chemiluminescence [28,29], and fluorescence signals [30,31], among which, electrochemical biosensors show merits of highly sensitive and selective, low cost, rapid and easy operation.

Herein, we have developed an electrochemical biosensor for highly sensitive detection of microRNAs based on the target recycling assisted

* Corresponding author.
** Corresponding author.
E-mail addresses: ian0126@126.com (Y. Yi), lijinlong1028@126.com (J. Li).
[1] Authors contributed equally to this work.

https://doi.org/10.1016/j.talanta.2020.121242
Received 29 May 2020; Accepted 3 June 2020
Available online 13 June 2020
0039-9140/

signal amplification strategy and the deposition of silver nanoparticles induced by streptavidin-biotin interaction. The hairpin (HP1) on the electrode can be opened by target miRNA-21. Next, HP2 are opened by the freshly exposed sticky end of HP1 and the target miRNA-21 are displaced. In the meantime, the released target miRNA hybridizes with another HP1, leading to more target cycles. Meantime, due to HP2 are modified with biotin, silver nanoparticles modified with streptavidin can bind with biotinized DNA (HP2). As a consequence, more biotinylated silver nanoparticles are deposited on the gold electrode surface through streptavidin-biotin interaction, which dramatically amplifies the electrochemical signal without the utilization of enzymes. In this design, the corresponding electrochemical signal is activated and enhanced in the presence of target miRNA. Therefore, the proposed biosensor has great potential as a platform for the ultrasensitive and selective detection of miRNAs.

2. Experimental

2.1. Chemicals and reagents

$NaBH_4$, biotin, $AgNO_3$, streptavidin, 6-Mercaptohexanol (MCH), trisodium citrate, and tris(carboxyethyl) phosphine (TCEP) were obtained from Sigma–Aldrich (Shanghai, China). The single stranded DNA or RNA oligonucleotides were obtained from Sangon Biotechnology Co., Ltd. (Shanghai, China). Their base sequences are listed as Table S1. The DNA solutions were prepared with 10 mM Tris-HCl buffer solution (pH 7.4) and the miRNAs solutions were prepared with DEPC-treated water. Blood samples were obtained from The Second Hospital of Nanjing, which were approved by the local Ethics Committee.

2.2. Exosomes isolation

Exosomes in blood samples were extracted according to the instructions of the exosome isolation kit (AIVD Biotech Co., ShenZhen, China). Then, the total RNA derived from exosomes was extracted by TRIzol reagent.

2.3. RT-qPCR analysis of miRNA-21

Firstly, total RNA derived from exosomes (4×10^{11} particles/mL) was extracted by TRIzol reagent according to the manufacturer's protocol and quantifed on a TU-1901 UV–vis spectrometer. Subsequently, a commercial Quant One Step qRT-PCR Kit was used as a control method (TIANGEN Biotech Co., Ltd., Beijing, China). Briefly, 50 μL of qRT-PCR reaction solution was prepared on ice (200 nM TaqMan probe, 250 nM forward primer, 200 nM RT primer, 250 nM reverse primer, 5 U of HotMaster Taq polymerase, 25 μL of 2 × Quant One Step Probe qRT-PCR Master Mix, 0.7 μL of Quant RTase, 5 μL of total RNA). Afterward, the above reaction solution was heated to 50 °C for 30 min. Finally, the detailed PCR reaction was operated according to the manufacturer's instructions.

2.4. Preparation of streptavidin modified silver nanoparticle and biotinylated AgNPs

Biotinylated AgNPs and streptavidin-AgNPs were prepared according to previous literature[32,33].

2.5. Electrochemical determination of miRNA-21

The gold electrode was treated as the previously report[34,35]. 2.0 μM HP1 in 10 μL of DNA immobilization buffer was dripped on the gold electrode overnight, and the surface density of HP1 was about 3.80×10^{-12} mol cm^{-2}. Then, after the above electrode was rinsed three times with DNA immobilization buffer and treated with 10 μL of Tris-HCl (10 mM), 1 mM MCH was used to react with the electrode for 15 min to avoid non-specific adsorption. Next, 10 μL PBS solution (10 mM, pH 7.4) containing various concentrations of miRNA-21 was cast on the gold electrode for 60 min at 37 °C. The above gold electrode was exposed to 50 μL of DNA hybridization solution containing 2.0 μM HP2 for 2 h at 37 °C. Later, the electrode was rinsed thoroughly with 10 mM Tris-HCl buffer and deionized water. The resulting clean electrode was immersed into 50 μL streptavidin-modified silver nanoparticles solution for 30 min at 37 °C and there were about 1.21×10^{-11} mol streptavidin on the gold electrode surface. Finally, after being dripped 10 μL of biotinylated AgNPs solution at 37 °C for half an hour, there were about 5.57×10^{-11} mol AgNPs left on the gold electrode surface, and the modified electrode was ready for measurement (Fig. S1).

2.6. Electrochemical measurements

Square wave voltammograms (SWV) and electrochemical impedance spectroscopy (EIS) were carried out on a CHI 660 E electrochemical workstation. The gold electrode (3 mm diameter), a saturated calomel electrode (SCE) and a platinum wire were served as the working electrode, reference electrode and counter electrode, respectively. SWV was obtained in 5 mL of 10 mM Tris-HNO_3 buffer (pH7.4) containing 100 mM KCl. EIS was performed in 5 mM $[Fe(CN)_6]^{3-/4-}$ solution containing 0.5 M KCl. The parameters of SWV and EIS were as follows: (a) SWV: scan range, −0.2 to 0.3 V; frequency, 15 Hz; sweeping rate, 0.25 V/s; step potential, 5 mV; amplitude, 25 mV; (b) EIS: amplitude, 5 mV; frequency range, 0.01Hz-100 KHz; bias potential, 0.22 V. The data was obtained at least three independent repetitions of the experiment.

3. Results and discussion

3.1. Mechanism of the method design

As shown in Scheme 1, the hairpin probes (HP1) are first modified on the gold electrode surface through Au–S. In the presence of target microRNAs, the stem-loop structure of HP1 can be opened via the combination with the target microRNAs. HP2 are opened by the freshly exposed sticky end of HP1 and the target miRNA is displaced when HP2 are dripped on the gold electrode surface. Meantime, the released miRNA further hybridizes with another HP1 and a set of reactions described above are recycled. Due to HP2 are modified with biotin, it can bind with silver nanoparticles modified with streptavidin. consequently, more biotinylated silver nanoparticles are deposited on the gold electrode through streptavidin-biotin interaction, resulting the enhanced electrochemical signals associated with concentrations of target miRNA.

3.2. Characterization of biotinylated AgNPs and streptavidin-AgNPs

Transmission electron microscope (TEM) is first selected to characterize the biotinylated AgNCs. As shown in Fig. 1A, the biotinylated AgNCs is spherical in shape, and the diameter is about 6 nm, which is accordance with previous reports. Moreover, the UV–vis spectrophotometry has been used to validate the modification of streptavidin to AgNPs. As shown in Fig. 1B, there is a strong absorbance peak at 280 nm for the UV–vis spectra of streptavidin-AgNPs compared with AgNPs. The results indicate that streptavidin-AgNPs complexes have been successfully synthesized.

3.3. Characterization of the electrode modification

EIS is used to verify the modification of the electrode (Fig. 2). EIS of the bare electrode is nearly a straight line (curve a, 43 Ω). After the modification of HP1 and MCH on the gold electrode surface, an evident semicircle appears (curve b, 1640 Ω), indicating augmented resistance

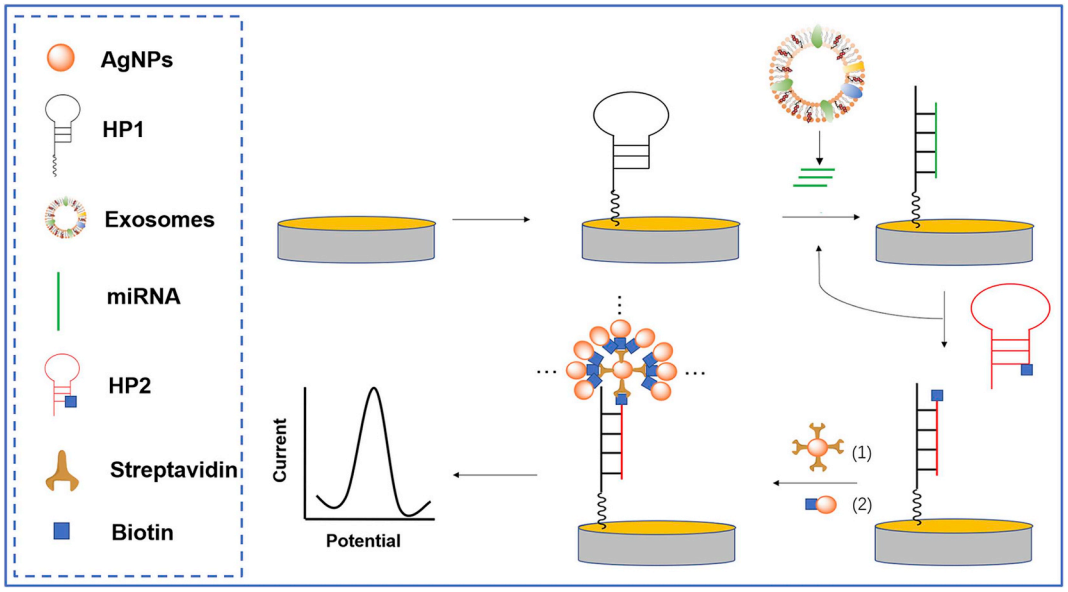

Scheme 1. Illustration of the electrochemical method for exosomal miRNA-21 assay.

to interface electron due to the repulsion of $[Fe(CN)_6]^{3-/4-}$ by the negatively charged DNA. The diameter of the semicircle increases remarkably after the hybridization between miRNA-21 and HP1 (curve c, 2253 Ω). Then, after addition of biotinylated HP2, the diameter of the semicircle increases with the combination of HP1 and biotinylated HP2 instead of miRNA hybridization (curve d, 3883 Ω). The diameter of the semicircle increases again after streptavidin-AgNPs are immobilized on the electrode through streptavidin-biotin interaction (curve e, 4988 Ω), ascribing to an electron transfer barrier caused by the combination between streptavidin and biotin. Finally, a larger semicircle diameter (curve f, 6012 Ω) is observed after the prepared biosensor being combined with biotinylated-AgNPs, due to the high resistance of the electrode interface, which indicates the successful fabrication of the biosensor.

3.4. Characterization of the biosensor

The signal amplification effect of streptavidin-biotin is verified by SWV. As is shown in Fig. 3, after streptavidin-biotin assisted signal amplification, the electrochemical signal is significantly enhanced. It can also be observed that the peak current response after signal amplification increases by about three times compared to no signal amplification.

3.5. Optimization of detection conditions

In order to obtain a better sensitivity of miRNA measurements, three important aspects involved in the assay have been examined. Firstly, the hybridization time between HP1 and miRNA-21 is optimized. It can be seen from Fig. S2, the SWV response increases with extention of catalytic hairpin assembly time and then reaches stabilization, and 60 min has been proved to be sufficient for completely hybridization. The hybridization time between HP1 and HP2 is also optimized. As shown in Figs. S3 and 2h has been proved to be the optimal incubation time. Besides these, streptavidin-biotin interaction time is also optimized for the amplification strategy in this assay. As shown in Fig. S4, the SWV response increases along the incubation time, and the signal tends to be constant after 30 min. So, an incubation time of 30 min has been selected for the signal amplification.

3.6. Electrochemical detection of miRNA-21

The level of synthetic miRNA-21 is analyzed using the electrochemical method mentioned above. As shown in Fig. 4, under the optimized conditions, the peak currents of AgNPs increase with the concentration of miRNA-21 ranging from 1 fM to 200 pM, and a limit of detection can be obtained as low as 0.4 fM (S/N = 3). The linear

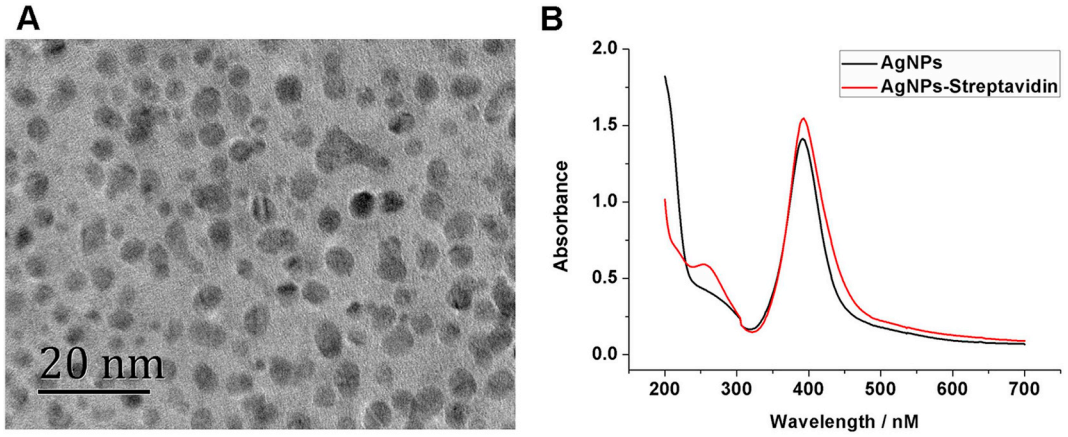

Fig. 1. (A) TEM image of biotinylated AgNPs; (B) UV–vis spectra of AgNPs and streptavidin-AgNPs.

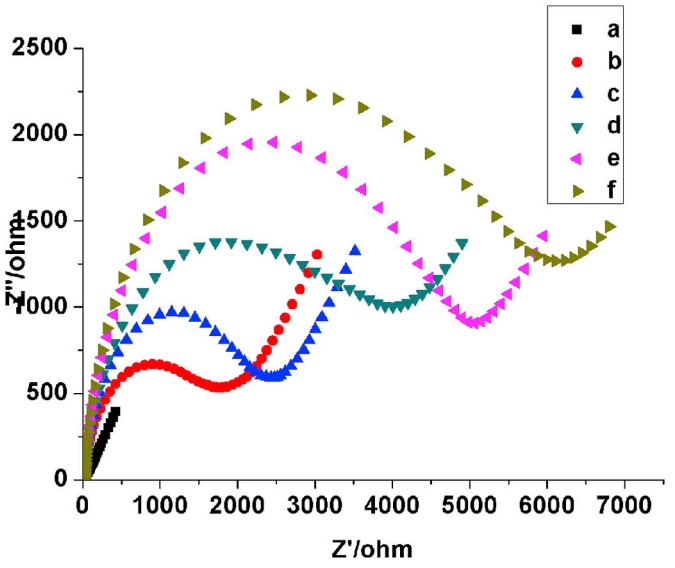

Fig. 2. EIS measurements for different modified electrodes: (a) bare gold electrode, (b) the electrode after HP1 modification, (c) the electrode after incubation with exosomal miRNA-21, (d) the electrode after incubation with biotinylated HP2, (e) the electrode after incubation with streptavidin-AgNPs, and (f) the electrode after incubation with biotinylated-AgNPs. (For interpretation of the references to colour in this figure legend, the reader is referred to the Web version of this article.)

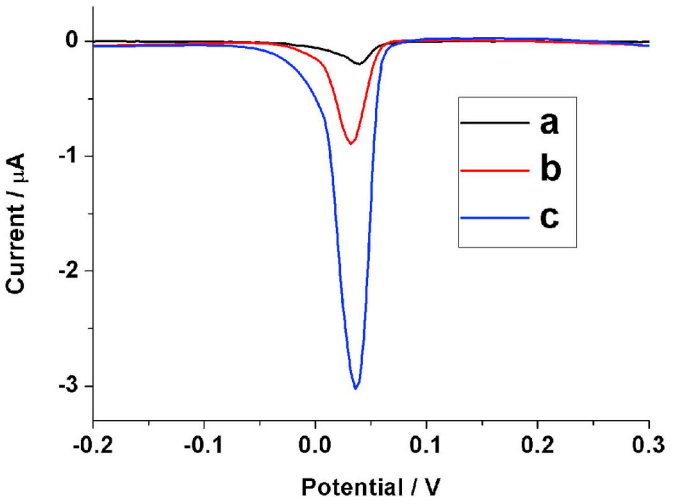

Fig. 3. SWV obtained at the modified electrodes of (a) streptavidin-AgNPs/miRNA-21/HP1/Au, and (b) biotinylated-AgNPs/streptavidin-AgNPs/miRNA-21/HP1/Au in 100 mM KCl containing 10 mM Tris-HNO_3, miRNA-21 concentration is 10 pM.

regression equation is y = −10.3–0.65x (n = 3, R^2 = 0.99). The reasons for the low detection limit are due to the following two signal amplification strategies. One is the released target miRNA can trigger a new cycle of catalytic assembly and more biotinylated HP2 can be immobilized on the gold electrode surface, which provides more binding sites for silver nanoparticles. The other is that a large number of silver nanoparticles can be aggregated on the electrode based on the streptavidin-biotin interaction.

3.7. Selectivity of the biosensor

We have compared the electrochemical biosensor performances in the cases of several miRNAs, such as miRNA-605, miRNA-200c and

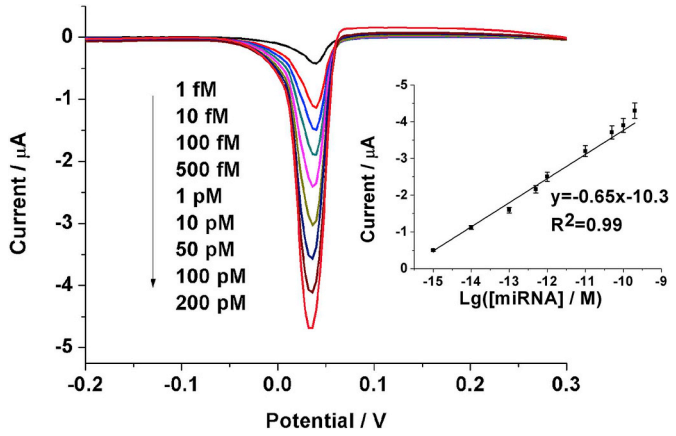

Fig. 4. (A) SWV curves obtained at the modified electrodes to quantify miRNA-21. Curves a-i corresponding to miRNA-21 concentrations of 0, 0.1, 0.5, 1, 10, 20, 50, 100, and 200 nM, respectively in 0.1100 mM KCl containing 10 mM Tris-HNO_3. The inset is the linear calibration curve of peak current value versus the logarithm of the concentration of exosomal miRNA-21. Error bars indicate standard deviation of three independent experiments.

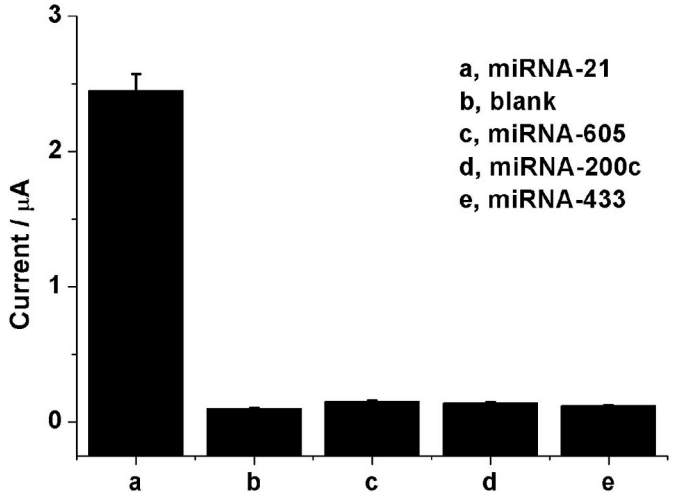

Fig. 5. Selectivity of the biosensor. Comparison of the SWV peak currents in the presence of miRNA-605, miRNA-200c, miRNA-433 and miRNA-21, respectively, in which the blank is PBS buffer. The concentrations of miRNA-21 and interfering miRNA are about 10 pM respectively. The error bars were the standard deviations from three independent experiments.

miRNA-433 to explore the selectivity of the biosensor. As shown in Fig. 5, high signal can be obtained only for the samples containing the target miRNA-21, while the electrochemical signals of the other miRNAs are close to the background level. That's reasonable since the other miRNAs cannot open the hairpin on the gold electrode surface and initiate the subsequent nanoparticle localization. The results indicate that the electrochemical biosensor has excellent specificity to distinguish target miRNA from the other miRNAs.

3.8. Assay exosomal miRNA-21 in biological sample

To further verify the potential of the proposed electrochemical biosensor in real blood samples analysis, we have also compared this method with qRT-PCR method. Exosomal miRNA-21 levels in serum samples derived from six prostatic cancer patients and six healthy volunteers are analyzed with the two methods. Firstly, the morphology and size of the exosomes are characterized by TEM and Dynamic Light Scattering (DLS) (Fig. 6). The TEM imaging results show that the

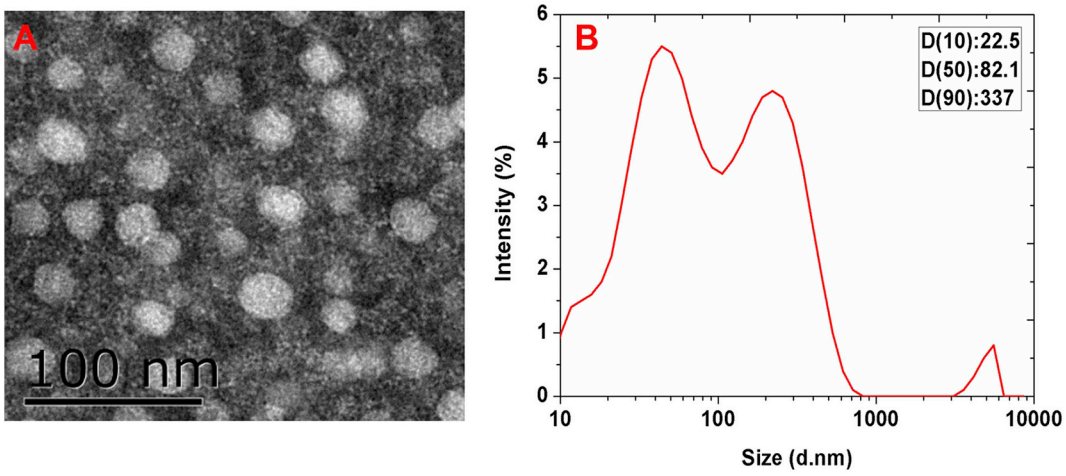

Fig. 6. (A) TEM image of exosomes extracted from blood samples of PCa patients; (B) Size distribution of exosomes by intensity.

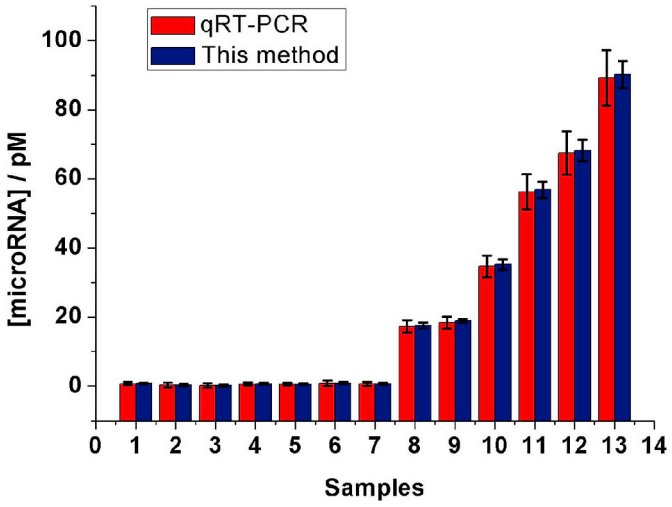

Fig. 7. Measurements of exosomal miRNA-21 levels in blood samples from patients with prostatic cancer patients (8–13) and healthy volunteers (2–7) by the proposed electrochemical method and qRT-PCR method; 1: blank control; The error bars represent the standard deviation of three independent experiments.

exosomes are globular structure with a particle diameter range of approximately 30–100 nm. Additionally, the DLS result displays a slightly larger range in diameter than that of TEM. Both the results of TEM and DLS are in agreement with the characteristics of exosomes described in previous literature. As can be seen in Fig. 7, the exosomal miRNA-21 levels are significantly higher in the samples from PCa patients than that from healthy volunteers, which indicates that exosomal miRNA-21 is over-expressed in tumor samples, consistent with previous literature. In addition, comparing the two methods, we can clearly see that they are in good consistency, which shows the high accuracy and practical application ability of our electrochemical method.

4. Conclusion

In summary, we have developed a sensitive electrochemical method for the detection of exosomal miRNAs in biological samples based on target recycling and streptavidin-biotin interaction assisted silver nanoparticles aggregation for signal amplification. Compared with other miRNA detection methods, our proposed electrochemical method exhibits three advantages. First, due to the double signal amplification strategy, the lower detection limit of 0.4 fM can be achieved to analyze miRNA-21 in human biological samples (Table 1). Second, the joint use of hairpin-like DNA probe and streptavidin-biotin interaction improves the specificity of this method. Third, this signal amplification strategy based on the deposition of AgNPs not only enables the miRNA detection with high sensitivity, but also easy to operate without the aid of enzyme. Moreover, the high consistency between our method and qRT-PCR validates that it could offer a useful means for the assay of exosomal miRNAs in biological samples.

Declaration of competing interest

The authors declare that they have no known competing financial interests or personal relationships that could have appeared to influence the work reported in this paper.

Acknowledgments

This work is supported by the National Natural Science Foundation of China (Grant No. 81703088) and the Medical Research Project of Jiangsu Provincial Health and Family Planning Commission, China (Grant No. H2018113).

Table 1
A comparison of the method with previously reported ones.

Detection method	Linear Range	Detection limit	Assay times	References
Surface enhanced Raman scattering	1 aM-100 nM	1 aM	Not provided	[24]
Surface enhanced Raman scattering	12 fM-18 pM	~5 fM	3.7 h	[36]
Surface enhanced Raman scattering	3 aM-100 pM	1 aM	50 min	[37]
Fluorescence	10 pM-10 nM	10 pM	2 h	[38]
Electrochemical	100 aM-1 nM	49 aM	2 h	[39]
Electrochemical	0.1 fM-100 fM	67 aM	3 h	[40]
Electrochemical	1 fM-200 pM	0.4 fM	3.5 h	This study

Appendix A. Supplementary data

Supplementary data to this article can be found online at https://doi.org/10.1016/j.talanta.2020.121242.

References

[1] G. Raposo, W. Stoorvogel, Extracellular vesicles: exosomes, microvesicles, and friends, JCB (J. Cell Biol.) 200 (4) (2013) 373–383.
[2] M. Colombo, G. Raposo, C. Thery, Biogenesis, secretion, and intercellular interactions of exosomes and other extracellular vesicles, in: R. Schekman, R. Lehmann (Eds.), Annual Review of Cell and Developmental Biology, 2014, pp. 255–289 30.
[3] K. Li, Y. Chen, A. Li, C. Tan, X. Liu, Exosomes play roles in sequential processes of tumor metastasis, Int. J. Canc. 144 (7) (2019) 1486–1495.
[4] S. Saeedi, S. Israel, C. Nagy, G. Turecki, The emerging role of exosomes in mental disorders, Transl. Psychiatry 9 (2019).
[5] Y. Guo, X. Ji, J. Liu, D. Fan, Q. Zhou, C. Chen, W. Wang, G. Wang, H. Wang, W. Yuan, Z. Ji, Z. Sun, Effects of exosomes on pre-metastatic niche formation in tumors, Mol. Canc. 18 (2019).
[6] L. Console, M. Scalise, C. Indiveri, Exosomes in inflammation and role as biomarkers, Clin. Chim. Acta 488 (2019) 165–171.
[7] E. Iranifar, B.M. Seresht, F. Momeni, E. Fadaei, M.H. Mehr, Z. Ebrahimi, M. Rahmati, E. Kharazinejad, H. Mirzaei, Exosomes and microRNAs: new potential therapeutic candidates in Alzheimer disease therapy, J. Cell. Physiol. 234 (3) (2019) 2296–2305.
[8] M. Mathieu, L. Martin-Jaular, G. Lavieu, C. Thery, Specificities of secretion and uptake of exosomes and other extracellular vesicles for cell-to-cell communication, Nat. Cell Biol. 21 (1) (2019) 9–17.
[9] L. Giannopoulou, M. Zavridou, S. Kasimir-Bauer, E.S. Lianidou, Liquid biopsy in ovarian cancer: the potential of circulating miRNAs and exosomes, Transl. Res. 205 (2019) 77–91.
[10] A.S. Aghabozorgi, N. Ahangari, T.E. Eftekhaari, P.N. Torbati, A. Bahiraee, R. Ebrahimi, A. Pasdar, Circulating exosomal miRNAs in cardiovascular disease pathogenesis: new emerging hopes, J. Cell. Physiol. 234 (12) (2019) 21796–21809.
[11] W. Geng, H. Tang, S. Luo, Y. Lv, D. Liang, X. Kang, W. Hong, Exosomes from miRNA-126-modified ADSCs promotes functional recovery after stroke in rats by improving neurogenesis and suppressing microglia activation, Am. J. Tourism Res. 11 (2) (2019) 780-+.
[12] W. Zhou, M.Y. Fong, Y. Min, G. Somlo, L. Liu, M.R. Palomares, Y. Yu, A. Chow, S.T.F. O'Connor, A.R. Chin, Y. Yen, Y. Wang, E.G. Marcusson, P. Chu, J. Wu, X. Wu, A.X. Li, Z. Li, H. Gao, X. Ren, M.P. Boldin, P.C. Lin, S.E. Wang, Cancer-secreted miR-105 destroys vascular endothelial barriers to promote metastasis, Canc. Cell 25 (4) (2014) 501–515.
[13] S. Manier, C.-J. Liu, H. Avet-Loiseau, J. Park, J. Shi, F. Campigotto, K.Z. Salem, D. Huynh, S.V. Glavey, B. Rivotto, A. Sacco, A.M. Roccaro, J. Bouyssou, S. Minvielle, P. Moreau, T. Facon, X. Leleu, E. Weller, L. Trippa, I.M. Ghobrial, Prognostic role of circulating exosomal miRNAs in multiple myeloma, Blood 129 (17) (2017) 2429–2436.
[14] S. Gholamin, A. Pasdar, M.S. Khorrami, H. Mirzaei, H.R. Mirzaei, R. Salehi, G.A. Ferns, M. Ghayour-Mobarhan, A. Avan, The potential for circulating microRNAs in the diagnosis of myocardial infarction: a novel approach to disease diagnosis and treatment, Curr. Pharmaceut. Des. 22 (3) (2016) 397–403.
[15] G.B. Andersen, J. Tost, Circulating miRNAs as Biomarker in Cancer, Recent results in cancer research. Fortschritte der Krebsforschung, Progres dans les recherches sur le cancer 215 (2020) 277–298.
[16] K. He, C. Guo, L. He, Y. Shi, MiRNAs of peripheral blood as the biomarker of schizophrenia, Hereditas 155 (2017) 1–5.
[17] A. Valoczi, C. Hornyik, N. Varga, J. Burgyan, S. Kauppinen, Z. Havelda, Sensitive and specific detection of microRNAs by northern blot analysis using LNA-modified oligonucleotide probes, Nucleic Acids Res. 32 (22) (2004).
[18] E. Berezikov, E. Cuppen, R.H.A. Plasterk, Approaches to microRNA discovery, Nat. Genet. 38 (2006) S2–S7.
[19] S.D. Fiedler, M.Z. Carletti, L.K. Christenson, Quantitative RT-PCR methods for mature microRNA expression analysis, Methods in molecular biology (Clifton, N. J. 630 (2010) 49–64.
[20] C.R.D. Chen, D.A. Ridzon, A.J. Broomer, Real-time quantification of microRNAs by stem-loop RT-PCR, Nucleic Acids Res. 33 (2005) 1–9.
[21] L.P. Lim, N.C. Lau, P. Garrett-Engele, A. Grimson, J.M. Schelter, J. Castle, D.P. Bartel, P.S. Linsley, J.M. Johnson, Microarray analysis shows that some microRNAs downregulate large numbers of target mRNAs, Nature 433 (7027) (2005) 769–773.
[22] E. Clancy, M. Burke, V. Arabkari, T. Barry, H. Kelly, R.M. Dwyer, M.J. Kerin, T.J. Smith, Amplification-free detection of microRNAs via a rapid microarray-based sandwich assay, Anal. Bioanal. Chem. 409 (14) (2017) 3497–3505.
[23] J. Zheng, J. Bai, Q. Zhou, J. Li, Y. Li, J. Yang, R. Yang, DNA-templated in situ growth of AgNPs on SWNTs: a new approach for highly sensitive SERS assay of microRNA, Chem. Commun. 51 (30) (2015) 6552–6555.
[24] J.U. Lee, W.H. Kim, H.S. Lee, K.H. Park, S.J. Sim, Quantitative and specific detection of exosomal miRNAs for accurate diagnosis of breast cancer using a surface-enhanced Raman scattering sensor based on plasmonic head-flocked gold nanopillars, Small 15 (17) (2019).
[25] M. Wang, Z. Fu, B. Li, Y. Zhou, H. Yin, S. Ai, One-step, ultrasensitive, and electrochemical assay of microRNAs based on T7 exonuclease assisted cyclic enzymatic amplification, Anal. Chem. 86 (12) (2014) 5606–5610.
[26] S. Xu, Y. Chang, Z. Wu, Y. Li, R. Yuan, Y. Chai, One DNA circle capture probe with multiple target recognition domains for simultaneous electrochemical detection of miRNA-21 and miRNA-155, Biosens. Bioelectron. 149 (2020).
[27] R. Salahandish, A. Ghaffarinejad, E. Omidinia, H. Zargartalebi, K. Majidzadeh-A, S.M. Naghib, A. Sanati-Nezhad, Label-free ultrasensitive detection of breast cancer miRNA-21 biomarker employing electrochemical nano-genosensor based on sandwiched AgNPs in PANI and N-doped graphene, Biosens. Bioelectron. 120 (2018) 129–136.
[28] X. Zhang, H. Liu, R. Li, N. Zhang, Y. Xiong, S. Niu, Chemiluminescence detection of DNA/microRNA based on cation-exchange of CuS nanoparticles and rolling circle amplification, Chem. Commun. 51 (32) (2015) 6952–6955.
[29] Y. Sun, L. Shi, Q. Wang, L. Mi, T. Li, Spherical nucleic acid enzyme (SNAzyme) boosted chemiluminescence miRNA imaging using a smartphone, Anal. Chem. 91 (5) (2019) 3652–3658.
[30] H. Liu, L. Li, Q. Wang, L. Duan, B. Tang, Graphene fluorescence switch-based co-operative amplification: a sensitive and accurate method to detection MicroRNA, Anal. Chem. 86 (11) (2014) 5487–5493.
[31] N. Wang, L. Song, Y. Qiu, H. Xing, J. Li, Hybridization-activated spherical DNAzyme for cascading two-photon fluorescence emission: applied for intracellular miRNA measurement by two-photon microscopy, Sensor. Actuator. B Chem. 286 (2019) 250–257.
[32] H. Li, Z. Sun, W. Zhong, N. Hao, D. Xu, H.-Y. Chen, Ultrasensitive electrochemical detection for DNA arrays based on silver nanoparticle aggregates, Anal. Chem. 82 (13) (2010) 5477–5483.
[33] J. Li, T. Gao, S. Gu, J. Zhi, J. Yang, G. Li, An electrochemical biosensor for the assay of alpha-fetoprotein-L3 with practical applications, Biosens. Bioelectron. 87 (2017) 352–357.
[34] J. Li, K. Hu, Z. Zhang, X. Teng, X. Zhang, Click DNA cycling in combination with gold nanoparticles loaded with quadruplex DNA motifs enable sensitive electrochemical quantitation of the tuberculosis-associated biomarker CFP-10 in sputum, Microchimica Acta 186 (2019).
[35] W. Cheng, J. Ma, Y. Zhang, C. Xu, Z. Zhang, L. Hu, J. Li, Bio-inspired construction of semi-artificial enzyme complex for detecting histone acetyltransferases activity, Analyst 145 (2019).
[36] D. Ma, C. Huang, J. Zheng, J. Tang, J. Li, J. Yang, R. Yang, Quantitative detection of exosomal microRNA extracted from human blood based on surface-enhanced Raman scattering, Biosens. Bioelectron. 101 (2018) 167–173.
[37] Y. Pang, C. Wang, L. Lu, C. Wang, Z. Sun, R. Xiao, Dual-SERS biosensor for one-step detection of microRNAs in exosome and residual plasma of blood samples for diagnosing pancreatic cancer, Biosens. Bioelectron. 130 (2019) 204–213.
[38] H.-W. Li, D. He, H. Luo, H. Wang, R. Wu, Enzyme-free quantification of exosomal microRNA by the target-triggered assembly of polymer DNAzyme nanostructure, Analyst 143 (2018).
[39] L. Liu, H. Lu, R. Shi, X.-X. Peng, Q. Xiang, B. Wang, Q.-Q. Wan, Y. Sun, F. Yang, G.-J. Zhang, Synergy of peptide-nucleic acid and spherical nucleic acid enabled quantitative and specific detection of tumor exosomal MicroRNA, Anal. Chem. 91 (20) (2019) 13198–13205.
[40] L.-L. Wang, M.-F. Hou, Y.-K. Xia, W.-H. He, A. Yan, Y.-P. Weng, L.-P. Zeng, J. Chen, A ratiometric electrochemical biosensor for the exosomal microRNAs detection based on bipedal DNA walkers propelled by locked nucleic acid modified toehold mediate strand displacement reaction, Biosens. Bioelectron. 102 (2017).